Published in final edited form as:
J Immunol. 2011 July 15; 187(2): 664–675. doi:10.4049/jimmunol.1100029.

Developmental arrest of T cells in RpL22-deficient mice is dependent upon multiple p53 effectors[1]

Jason E. Stadanlick[*,¶], **Zhiqiang Zhang**[*,¶], **Sang-Yun Lee**[*], **Mike Hemann**[†], **Matthew Biery**[&], **Michael O. Carleton**[&], **Gerard P. Zambetti**[‡], **Stephen J. Anderson**[§], **Tamas Oravecz**[§], and **David L. Wiest**[*,2]

[*]Immune Cell Development and Host Defense Program, Blood Cell Development and Cancer Keystone, Fox Chase Cancer Center, 333 Cottman Avenue, Philadelphia, PA 19111

[†]Massachusetts Institute of Technology, Department of Biology, 40 Ames Street, E17-128B, Cambridge MA 02139

[&]Rosetta Inpharmatics LLC, 401 Terry Ave. N, Seattle WA 98109

[‡]Department of Biochemistry, St. Jude Children's Research Hospital, 262 Danny Thomas Place Memphis, TN 38105-3678

[§]Department of Immunology, Lexicon Pharmaceuticals, Inc., 8800 Technology Forest Place, The Woodlands, TX 77381

Abstract

αβ and γδ lineage T cells are thought to arise from a common $CD4^{-}CD8^{-}$ progenitor in the thymus. However, the molecular pathways controlling fate selection and maturation of these two lineages remain poorly understood. We have demonstrated recently that a ubiquitously expressed ribosomal protein, Rpl22, is selectively required for the development of αβ lineage T cells. Germline ablation of Rpl22 impairs development of αβ lineage, but not γδ lineage, T cells through activation of a p53-dependent checkpoint. In this study, we investigate the downstream effectors employed by p53 to impair T cell development. We found that many p53 targets were induced in *Rpl22*$^{-/-}$ thymocytes, including miR-34a, PUMA, $p21^{waf}$, Bax, and Noxa. Notably, the pro-apoptotic factor Bim, while not a direct p53 target, was also strongly induced in *Rpl22*$^{-/-}$ T cells. Gain-of-function analysis indicated that overexpression of miR-34a caused a developmental arrest reminiscent of that induced by p53 in Rpl22-deficient T cells; however, only a few p53 targets, when individually ablated by gene targeting or knockdown, alleviated developmental arrest. Co-elimination of PUMA and Bim resulted in a nearly complete restoration of development of *Rpl22*$^{-/-}$ thymocytes, indicating that p53-mediated arrest is enforced principally through effects on cell survival. Surprisingly, co-elimination of the primary p53 regulators of cell cycle arrest ($p21^{waf}$) and apoptosis (PUMA) actually abrogated the partial rescue caused by loss of PUMA alone, suggesting that the G1 checkpoint protein $p21^{waf}$ might actually facilitate thymocyte development in some contexts.

[1]This work was supported by NIH grants R01AI073920, R21CA141194, NIH core grant P01CA06927, Center grant P30-DK-50306, and an appropriation from the Commonwealth of Pennsylvania. JES and SYL were supported by the Fox Chase Cancer Center NIH Postdoctoral Training Grant (T32 CA00903534 and F32 AI089077-01A1) and Greenwald Postdoctoral Fellowship, respectively.

[2]To whom correspondence should be addressed: David L. Wiest, Fox Chase Cancer Center, R364, 333 Cottman Avenue, Philadelphia, PA 19111, Tel: 215-728-2966, Fax: 215-728-2412, david.wiest@fccc.edu.
[¶]These authors contributed equally to the work

Introduction

Development of αβ-lineage T cell progenitors from the $CD4^{-}CD8^{-}$ double negative (DN)3 stage to the $CD4^{+}CD8^{+}$ double positive (DP) stage requires traversal of the β-selection checkpoint, which ensures that only progenitors that have productively rearranged the T cell receptor (TCR) β locus will survive. DN thymocytes can be further subdivided based upon the surface expression of CD25 and CD44 into four subsets: DN1, $CD44^{+}CD25^{-}$; DN2, $CD44^{+}CD25^{+}$; DN3, $CD44^{-}CD25^{+}$; and DN4, $CD44^{-}CD25^{-}$. TCRβ rearrangement is initiated as thymocytes develop from the DN2 to the DN3 stage. If during this transition rearrangement of the TCRβ locus fails to preserve the translational reading frame of TCRβ, the cells die by apoptosis (1); however, if the translational reading frame is preserved and produces a functional TCRβ protein, it assembles with the remaining subunits of the pre-T cell receptor (pre-TCR) complex (pre-Tα, along with CD3γ, δ, ε, and ζ) and transduces ligand-independent signals, resulting in a number of developmental outcomes including termination of TCRβ rearrangement (i.e., allelic exclusion), rescue from cell death, proliferation, and differentiation to the DP stage (2, 3). The pre-TCR complex orchestrates these developmental outcomes by regulating the expression or function of numerous transcription factors including early growth response genes (Egr1–3) and NF-ATc, which cooperatively yield increased expression of inhibitor of DNA binding 3 (ID3) and traversal of the β-checkpoint (4–6).

We recently made the surprising finding that the ribosomal protein L22 (Rpl22) is required for traversal of the β-selection checkpoint and so also appears to be an important molecular effector of the developmental outcomes orchestrated by pre-TCR signaling (7). Rpl22 is a ubiquitously expressed RNA binding protein that is a component of the 60S ribosomal subunit but is not essential for global or CAP-dependent translation (8, 9). Strikingly, Rpl22 ablation does not affect health or size of the mice yet does result in a profound T lymphopenia, with most αβ lineage T cells arresting at the β-selection checkpoint at the DN3 stage (7). The developmental arrest at the DN3 stage in Rpl22-deficient mice results from an αβ lineage-restricted induction of the p53 tumor suppressor, as epistasis analysis reveals that the developmental arrest is completely alleviated by eliminating p53 through gene ablation (7). Interestingly, p53 induction in Rpl22-deficient DN3 cells appears to result from increased translation, implicating Rpl22 as a regulator of p53 synthesis. Other ribosomal protein defects have been implicated in impairing hematopoietic cell development (e.g., RpS19 mutations disrupting erythroid development in Diamond-Blackfan Anemia) (10); however, no ribosomal protein mutations had previously been shown to selectively impair T cell development (11).

While ribosomal proteins are critical components of cellular ribosomes on which all proteins are synthesized, an increasing number of reports have revealed additional roles for ribosomal proteins in regulating fundamental cellular processes, such as survival, from outside of the ribosome (12). Among these extraribosomal functions is the regulation of p53 expression. For example, ribosomal protein S7 that fails to be incorporated into ribosomes because of impaired small ribosomal subunit assembly, enhances the translation of the ribosomal protein L11 (Rpl11), which in turn, activates p53 by preventing its degradation by the ubiquitin ligase MDM2 (13). Likewise, ribosomal proteins Rpl5 and Rpl23 are also able to activate p53 by binding to and impairing MDM2 function upon being released from the nucleolus under conditions of nucleolar stress (14, 15). Finally, Rpl26 is able to directly increase the rate of p53 synthesis via binding to the 5′ untranslated region (UTR) of p53

[3]Abbreviations: DN, double negative; DP, double positive; TCR, T cell receptor, pre-TCR, pre-T cell receptor; RpL22, ribosomal protein L22; BH3, Bcl-2-homology domain 3-only; Bax, Bcl-associated-X protein; Noxa, NADPH oxidase activator 1; PUMA, p53-upregulated modulator of apoptosis

mRNA (16, 17). Therefore, while some ribosomal proteins control p53 by regulating its stability, other ribosomal proteins (Rpl26 and Rpl22) do so by altering p53 translation (7, 13).

The tumor suppressor p53 regulates a complex and multi-layered network of pro-apoptotic and cell cycle inhibitory factors and mediates life or death decisions in response to stresses. One way in which p53 activation regulates survival is through the transcriptional induction of pro-apoptotic Bcl-2-homology domain 3-only (BH3) family of proteins (18). This family of proteins includes Bcl-associated X protein (Bax), NADPH oxidase activator 1 (Noxa), and p53-upregulated modulator of apoptosis (PUMA). An additional BH3-only family member, Bim, that is not a direct p53 target, is nevertheless induced in T cells in response to stresses such as cytokine withdrawal and DNA damage and ultimately leads to compromised mitochondrial integrity and apoptosis (19, 20). Several of these proteins have been identified as critical effectors of p53-mediated apoptosis or growth arrest. PUMA-deficient T cells are highly resistant to UV and chemical-induced apoptosis, despite large increases in p53 protein (21). Similarly, Bim or Noxa-deficient T cell precursors or MEF cells exhibited enhanced resistance to cell death in response to similar stimuli (19, 22, 23). In addition to its role in regulating cell survival, p53 can also control cell-cycle progression via the G1 checkpoint protein $p21^{waf}$, which allows for reversible cell cycle arrest in the event of DNA damage (24–26) or for a permanent arrest through activation of an oncogene-induced senescence program. In addition to the transactivation of particular downstream regulators of growth or survival, p53 can also induce the micro-RNA miR-34a, which is able to regulate a large battery of individual p53 effectors and is thereby able to replicate many of the consequences of p53 induction, including G1 arrest and apoptotic cell death (27).

Many downstream targets are induced upon p53 activation, but the particular effectors responsible for the diverse developmental outcomes differ depending on the stimulus responsible for p53 induction. For example, PUMA orchestrates thymocyte death in response to DNA damage, whereas Noxa is more important in the context of oncogene activation (28). While our observations indicated a link between Rpl22 and p53 protein expression in developing αβ lineage T cells, the p53 targets responsible for the arrest of thymocyte development were unknown. Herein we identify the targets upregulated following p53 activation in Rpl22-deficient αβ-lineage precursors and then assess their role in the resulting p53-mediated developmental block. We found that many direct targets of p53 activation were induced, including miR-34a, PUMA, $p21^{waf}$, Bax, and Noxa, as well as the pro-apoptotic BH3 only gene Bim, which is not considered to be a direct p53 target. Interestingly, while gain-of-function analysis indicated that overexpression of miR-34a is sufficient to impair development in a similar fashion to that observed following p53 induction in Rpl22-deficient T cells, few pro-apoptotic factors (PUMA and Bim) exerted sufficiently potent effects such that development was detectably rescued by their individual elimination. Importantly, co-elimination of the pro-apoptotic factors, PUMA and Bim, resulted in a nearly complete rescue of the development of $Rpl22^{-/-}$ thymocytes. In contrast, simultaneous elimination of the primary p53 regulators of cell cycle arrest ($p21^{waf}$) and apoptosis (PUMA) actually afforded less rescue in terms of cell frequency and cellularity than ablation of PUMA alone, suggesting that loss of the G1 checkpoint protein $p21^{waf}$ renders thymocytes more sensitive to arrest by other p53 effectors.

Materials and Methods

Mice

All mouse strains were housed in the Association for Assessment and Accreditation of Laboratory Animal Care-accredited Laboratory Animal Facility at Fox Chase and were handled in accordance with Institutional Animal Care and Use Committee approved

protocols. The following mouse strains were used: Rpl22-deficient (7); PUMA-deficient (21); Rag2-deficient (29); $p21^{waf}$-deficient (Jackson Research Laboratories, Bar Harbor, ME)(24); pre-Tα-deficient (A generous gift of Dr. H von Boehmer, Dana Farber Cancer Institute)(30); and p53-deficient (A generous gift of Dr. Maureen Murphy, Fox Chase Cancer Center)(31). Genotypes were confirmed performing PCR analysis on tail DNA at weaning and again prior to use in experiments.

Quantitative real-time PCR

Total RNA was isolated from primary cells using the RNA-Easy system (Qiagen, Valencia, Ca). Purified mRNA was converted to cDNA using Superscript II reverse transcription PCR with oligo $dT_{(12–18)}$ primers (Invitrogen, Carlsbad, CA). Quantitative real-time PCR was performed on the Prism 7700 thermocycler (Applied Biosystems, Carlsbad, CA) using Taqman Real-time PCR primer/probe sets specific to murine PUMA/*Bbc3* (Mm00519268_m1), Noxa/*Pmaip1* (Mm00451763_m1), and Bim/(*Bcl2l-11*) (Mm01333921_m1). $P21^{waf}$/*Cdkn1a* and *Bax* primer/probe sets were custom generated by the Fox Chase Cancer Center Genomics Core Facility. miR RNA was isolated using the miR Easy system in conjunction with the RNeasy MinElute Cleanup Kit (Qiagen, Valencia, CA). Isolated RNA was converted to cDNA by the Multiscribe RT-PCR kit (Applied Biosystems). miR expression was determined by the Taqman Micro RNA assay for miR-34a and sno-202. Real-time PCR was performed as indicated above.

Anti-CD3 treatment

Mice were injected intraperitoneally with affinity column purified anti-CD3 (145-2C11) at 10μg/g body weight in a total volume of 200μL of PBS per mouse or were injected with PBS alone. Mice were then harvested at the indicated times. For each experiment, 4 mice received PBS (control) treatment and 2 mice/time point received anti-CD3 injection. $CD4^{-}CD8^{-}CD44^{-}$ (DN3+DN4) thymocytes were isolated by cell sorting and used to generate cDNA for real-time PCR analysis or to produce detergent extracts for immunoblotting.

Immunoblot analysis

Cells were lysed in NP-40 Lysis Buffer (1% NP-40, 50mM TRIS pH 8.0, 150mM NaCl) with a complete mini-tab inhibitor tablet. Samples were resolved on NuPage Novex Bis-Tris gels (Invitrogen) and blotted with the following antibodies: anti-p53 (Clone #IMX25, Leica Microsystems, UK), anti-Bim/BOD (Clone AAP-330, Assay Designs Inc., Ann Arbor, MI), anti-Noxa (FL-103, Santa Cruz Bio., CA), anti-myc tag (EQKLISEEDL) and anti-Bax (Cell Signaling Technologies, Beverly, MA).

OP9 cell cultures and shRNA retroviral transduction

Viral particles were produced by transient calcium-phosphate transfection of Phoenix cells with shRNAs expressed in the MSCV-based vectors, LMP or LMS, as described (32). Fetal livers were harvested on day 14 of gestation and genotyped as described above. Hematopoietic precursors were expanded on OP9-DL1 expressing monolayers containing IL7 (5ng/mL) and Flt-3 (5ng/mL). After four days, cells were spin-infected with retrovirus containing shRNA targeting Bax (MLS-Bax), Bim (MLS-Bim), Noxa (MLS-Noxa), or an irrelevant control (MLS-T-1052). For p53 knockdown, precursors were infected with a control vector (LMP) or LMP-p53 (provided by S. Lowe, Cold Spring Harbor Laboratory). Cells were cultured for the indicated times and analyzed by flow cytometry.

Flow cytometric analysis

Single cell suspensions of thymic cells were stained with antibodies to CD4 (clone GK1.5), CD25 (clone 7D4), CD44 (clone IM7), γδTCR (clone GL3), and CD8 (Clone 53-6.7) (BioLegend, San Diego, CA). For cell death assays, cells were stained with Annexin-V PE (BD Biosciences, San Jose, CA). Data were collected using the LSRII (BD Biosciences, San Jose, CA) and were analyzed using FlowJo software (Tree Star, Ashland, OR).

Myc-tagged Noxa construct

Two consecutive Myc-Tag sequences encoding EQKLISEEDL were appended to the 5′ end of the Noxa mRNA sequence, along with the relevant 3′ UTR binding region for the Noxa shRNA. The PCR-generated product was directionally cloned into PMIY dsCherry II and then used to generate virus for stable retroviral transduction into Scid.adh cells. Cells transduced with either control shRNA or Noxa shRNA were sorted for GFP expression and used in Immunoblot analysis for Myc-tag expression (anti-Myc Tag (71D10), Cell Signaling Technologies, MA).

Cell cycle analysis

Cell cycle analysis was performed using the FITC BrdU Flow Kit (BD Pharmingen, San Jose, CA). Briefly, mice were injected intraperitoneally with 1mg/mL of BrdU in sterile PBS and rested for 4 h prior to harvesting. Thymocytes were surface stained with T cell markers then fixed and permeabilized with BD Cytofix/Cytoperm buffer. Each sample was treated with 30μg DNAse for 1 h prior to intracellular staining with anti-BrdU FITC and 7-amino-actinomycin D (7-AAD) and analysis on the LSR II.

Results

Trp53 ablation restores development of RpL22-deficient αβ-lineage T cells

Germline ablation of the *Rpl22* gene in mice results in a severe T lymphopenia caused by selective impairment of αβ-lineage T cell development in the thymus, with few T cell precursors maturing beyond the $CD4^{-}CD8^{-}$ DN stage (Figure 1A). Further subsetting of DN thymocytes based on differential expression of CD44 and CD25, revealed that the developmental block occurs at the $CD44^{-}CD25^{+}$ DN3 stage (Figure 1B). The impairment in T cell development in $Rpl22^{-/-}$ mice was associated with increased apoptosis, as indicated by elevated Annexin V binding in the majority of T cell subsets (Figure 1C). Interestingly, the developmental blockade was preferentially manifested in αβ lineage precursors, as development of γδ lineage cells was only mildly impaired (Figure 1B). Previous analysis had revealed that the development of Rpl22-deficient thymocytes is impaired by activation of a p53-dependent checkpoint (7). Indeed, development of Rpl22-deficient thymocytes is completely restored by p53 deficiency, as illustrated by the total and complete rescue of T cell development in $Rpl22^{-/-}Trp53^{-/-}$ mice. These mice demonstrated both restored thymic cellularity and representation of T cell populations (Figure 1A and B) as well as reduced apoptosis (Figure 1C).

The developmental arrest of T cell development in $Rpl22^{-/-}$ mice is associated with the induction of multiple p53 effectors

The relative resistance of developing γδ lineage cells to Rpl22-deficiency results from the absence of p53 induction in these cells (7). Accordingly, we compared the expression of p53 effector molecules in αβ and γδ lineage precursors to gain insight into those responsible for the observed developmental block. We performed quantitative real-time PCR analysis on sorted αβ-lineage DN3 and γδ T cells from $Rpl22^{+/+}$ and $Rpl22^{-/-}$ mice as well as from pre-Tα-deficient ($Ptcra^{-/-}$) mice, which are similarly arrested at the DN3 stage, albeit by a

distinct mechanism (33, 34). We observed a 2 to 6-fold increase in both cell cycle arrest and pro-apoptotic factors in *Rpl22*$^{-/-}$ αβ-lineage thymocytes, including p21^{waf}, Bax, Bim, and PUMA, and a consistently robust increase in Noxa (Figure 2). The increased expression of p21^{waf} and the pro-apoptotic factors was restricted to *Rpl22*$^{-/-}$ αβ-lineage cells, as it was not observed in either *Rpl22*$^{-/-}$ γδ lineage cells or in *Ptcra*$^{-/-}$ mice, where the developmental arrest results from the absence of pre-TCR signaling (30). Finally, we did observe Noxa induction in *Rpl22*$^{-/-}$ γδ lineage cells, but to a much lesser extent than in *Rpl22*$^{-/-}$ αβ lineage DN3 cells (Figure 2). Taken together, these data suggest that the impairment in αβ lineage T cell development in Rpl22-deficient mice is correlated with induction of numerous direct and indirect p53 targets capable of inducing cell cycle arrest (p21^{waf}) and apoptosis (Bax, Noxa, PUMA, and Bim).

Developing T lineage precursors that undergo apoptosis in the thymus are rapidly cleared by phagocytosis (35). Accordingly, it is possible that the expression analysis in Figure 2 could have been affected by the relative efficiency with which different populations are phagocytically removed. In an attempt to mitigate this concern, we employed a model system in which the traversal of the β-selection checkpoint could be induced in a synchronous fashion, using anti-CD3 stimulation of pre-TCR deficient (Rag2-deficient) thymocytes (36). Rag2-deficient thymocytes that were either *Rpl22*$^{+/+}$ or *Rpl22*$^{-/-}$ were stimulated in vivo by intraperitoneal injection with anti-CD3 antibody, which mimics a pre-TCR stimulus and induces thymocytes to mature from the DN3 to the CD44^{-}CD25^{-} DN4 stage within 24 h (36) (Figure 3A). We observed that by 24 h after stimulation, the extent of CD25 down modulation was beginning to lag in the *Rpl22*$^{-/-}$ mice, even though both *Rpl22*$^{+/+}$ and *Rpl22*$^{-/-}$ thymocyte populations had received equivalent stimulation, as shown by identical induction of CD5, an indicator of signal intensity (37) (Figure 3A). *Rpl22*$^{-/-}$ thymocytes exhibited elevated levels of p53 protein even before anti-CD3 stimulation that were robustly induced upon anti-CD3 treatment (Figure 3B). Taken together, these data indicate that the induction of p53 began to manifest as a developmental arrest by 24 h post stimulation (Figure 3A,B). Surprisingly, we also observed a modest induction of p53 in anti-CD3 stimulated *Rpl22*$^{+/+}$ thymocytes (Figure 3B); moreover, it was transient, as it abated by 48 h in *Rpl22*$^{+/+}$ but not *Rpl22*$^{-/-}$ thymocytes, where its sustained expression leads to cell death (Figure 3B). The cause of p53 induction in anti-CD3 stimulated *Rpl22*$^{+/+}$ thymocytes is not clear, but could be due to a transient stress response associated with the extensive proliferation caused by this mitogenic signal. Having identified an early stage in the p53-mediated developmental block of *Rpl22*$^{-/-}$ thymocytes (24 h), we performed quantitative real-time PCR analysis to determine whether the set of p53 effectors induced under these conditions was similar to those above. Indeed, as in asynchronously developing *Rpl22*$^{-/-}$ thymocyte populations, we found 2 to 6-fold increases in expression of the pro-apoptotic factors PUMA, Bax, and Noxa as compared to PBS treated *Rpl22*$^{+/+}$ cells (Figure 3C). In contrast to what we observed in asynchronously developing *Rpl22*$^{-/-}$ thymocytes (Figure 2), expression of p21^{waf1} and Bim decreased in both the anti-CD3 stimulated *Rpl22*$^{+/+}$ and *Rpl22*$^{-/-}$ cells (Figure 3C). Currently, the basis for this difference in p21^{waf} and Bim expression between mitogenically stimulated and asynchronously developing *Rpl22*$^{-/-}$ thymocytes is unknown, however this may reflect a temporal delay in induction relative to that of other p53 targets.

Expression of miR-34a arrests thymocyte development

miRs are small noncoding RNAs that can regulate gene expression by altering mRNA stability or translation (27, 38, 39). miR-34a was recently identified as a direct p53 target, whose induction is capable of independently replicating many of the effects of p53 activation, including G1 arrest and apoptosis (27). Therefore, we asked if miR-34a were induced by p53 in RpL22-deficient thymocytes. Indeed, both control *Rag2*$^{-/-}$*Rpl22*$^{-/-}$ cells

and those stimulated to differentiate with anti-CD3 exhibited a 2-fold increase in miR-34a expression over control treated RpL22-sufficient T cells (Figure 4A). Since miR-34a is induced in Rpl22-deficient T cells, we asked if miR-34a expression alone was sufficient to replicate the effects of p53 induction and arrest T cell development. To address this question, we used a gain-of-function approach by retrovirally transducing miR-34a into adult DN thymocytes and monitoring development in OP9-DL1 stromal cell cultures. OP9-DL1 cells support the development of immature T cells up through the DP stage in vitro (40). Cells transduced with empty vector or mutant miR-34a (MIR34M) displayed a marked increase in the number of T lineage precursors that had developed to the immature DP stage between days 1 and 4 (Figure 4B). Conversely, transduction with miR-34a significantly impaired development to the DP stage, both regarding the frequency and number of cells (Figure 4B, C). Our findings suggest that induction of the p53 target miR-34a plays an important role in the p53-mediated blockade of T cell development in *Rpl22*$^{-/-}$ mice.

Ablation of the *Cdkn1a* gene encoding p21^{waf} fails to alleviate the developmental blockade of RpL22-deficient αβ T cells

Since gain-of-function analysis revealed that enforced expression of miR-34a caused a developmental arrest reminiscent to that resulting from p53 activation in *Rpl22*$^{-/-}$ thymocytes, we asked if loss-of-function analysis would reveal which of the induced p53 effectors might play a sufficiently important role that their individual ablation alleviates the developmental block. p53 activation induces targets that fall into two broad functional classes: those that regulate cell growth and those that regulate survival. Among these factors, the most frequently implicated in regulating cell growth and survival are p21^{waf} and PUMA, respectively (21, 24, 41). Because both of these p53 targets are induced in *Rpl22*$^{-/-}$ thymocytes (Figures 2 and 3C), we employed loss-of-function analysis to investigate their importance in the p53-mediated impairment of thymocyte development. Specifically, we assessed whether p21^{waf}-deficiency (i.e., *Cdkn1a* ablation) would alleviate the development block and restore development of *Rpl22*$^{-/-}$ thymocytes to the DP stage. Surprisingly, rendering Rpl22-deficient thymocytes deficient for p21^{waf} (*Rpl22*$^{-/-}$*Cdkn1a*$^{-/-}$) failed to alleviate the developmental arrest, as the vast majority of thymocytes remained at the DN stage, primarily at the β-selection checkpoint at DN3, just as in p21^{waf}-expressing *Rpl22*$^{-/-}$ mice (Figure 5A,B). Moreover, p21^{waf}-deficiency did not suppress the increased apoptosis routinely observed in Rpl22-deficient thymocytes (Figure 5C). These data indicate that elimination of p21^{waf} alone was not sufficient to restore development of *Rpl22*$^{-/-}$ thymocytes, perhaps because pro-apoptotic p53 targets were still present and might be inducing cell death.

PUMA-deficiency suppresses p53-mediated apoptosis and partially restores development of RpL22-deficient thymocytes

Since ablation of the cell cycle regulator p21^{waf} failed to rescue development, we attempted to rescue the p53-mediated developmental arrest by disabling apoptotic pathways. PUMA is a pro-apoptotic BH3 family member and a major p53-activated inducer of apoptosis, whose ablation can abrogate p53-mediated death induced by cellular insults/stressors, including γ-irradiation, dexamethasone, or cytokine withdrawal (21). We therefore asked whether PUMA-deficiency would alleviate the p53-induced developmental block of *Rpl22*$^{-/-}$ thymocytes. Indeed, relative to mice singly deficient for Rpl22, those doubly-deficient for both PUMA and Rpl22 exhibited a significant increase in both the frequency and absolute number of thymocytes that developed to the DP stage (Figure 6A). Nevertheless, this represented only a partial rescue, returning thymic cellularity to only approximately 10% of wild type levels (Figure 6A) and failing to cause a significant increase in the absolute number of cells that have developed beyond the DN3 stage to DN4 stage cells (Figure 6B). Finally, an examination of cell viability by Annexin V staining indicated that while PUMA

deletion substantially reduced the level of apoptosis in nearly all T cell subsets, it appeared that the suppression of apoptosis was incomplete, as indicated by the elevated apoptosis manifested in total *Rpl22*$^{-/-}$*Puma*$^{-/-}$ thymocytes and the CD4 SP thymocyte subsets, relative to littermate controls (Figure 6C). Taken together, these data indicate that PUMA plays an important role in the p53-mediated promotion of apoptosis in *Rpl22*$^{-/-}$ thymocytes; however, unlike thymocyte apoptosis following γ-irradiation which is fully rescued by PUMA deficiency (21), the apoptosis accompanying Rpl22-deficiency appears to involve additional pro-apoptotic effectors.

To determine whether pro-apoptotic effectors other than PUMA were contributing to the death of *Rpl22*$^{-/-}$ thymocytes, we investigated the other death effectors identified in our expression analysis (Bax, Bim, and Noxa; Figure 2). Their role in the developmental block of *Rpl22*$^{-/-}$ thymocytes was examined by knocking down their expression in *Rpl22*$^{-/-}$ fetal progenitors and monitoring the effect on development on OP9-DL1 monolayers as was done for adult progenitors in Figure 4. Analysis was restricted to GFP^{+} cells that had been transduced with the shRNA retroviral vector (MLS)(32). A comparison of GFP^{+} cells reaching the DP stage in shRNA-treated versus the control shRNA-expressing cells reveals the extent to which knockdown of the the death effectors blunts p53-mediated apoptosis and alleviates the developmental blockade of αβ lineage *Rpl22*$^{-/-}$ thymocytes (Figure 7). Knockdown of p53 in *Rpl22*$^{-/-}$ progenitors restored development to about half the level observed in control-transduced *Rpl22*$^{+/+}$ progenitors and was used to normalize results from knockdown of pro-apoptotic effectors (Figure 7A). Surprisingly, while expression of multiple pro-apoptotic effectors was induced in *Rpl22*$^{-/-}$ thymocytes (Bim, Noxa, and Bax), knocking down the expression of Noxa and Bax failed to alleviate the developmental blockade and promote development to the DP stage (Figure 7A and C); however, knockdown of Bim did result in a partial rescue of development, restoring development approximately half as effectively as did knocking down p53 (Figure 7A). Importantly, when Bim was knocked down in *Rpl22*$^{-/-}$*Puma*$^{-/-}$ T cells, the rescue of development to the DP stage was nearly equivalent to that resulting from knocking down p53 itself (defined as 100%: Figure 7B and C). In summary, our loss-of-function analysis of pro-apoptotic factors suggests that Bim and PUMA play significant roles in p53-mediated developmental blockade, while Bax and Noxa do not, despite the very large induction in Noxa expression.

PUMA/p21^{waf} double-deficiency fails to cooperate in alleviating developmental block of *Rpl22*$^{-/-}$ T cell progenitors

Our analysis of the roles of pro-apoptotic effectors revealed that the combined elimination of Bim and PUMA resulted in nearly complete rescue of development, suggesting that simultaneous elimination of other p53 effectors might be informative. Since p53 regulates both cell cycle through p21^{waf} and apoptosis through PUMA and Bim, we asked how simultaneously disabling p53's ability to mediate cell cycle arrest (p21^{waf}-deficiency) and promote apoptosis (PUMA-deficiency) would affect development of Rpl22-deficient progenitors. That is, we asked whether Rpl22/PUMA/p21^{waf} triple-deficiency would more completely rescue development. Surprisingly, we observed that p21^{waf}-deficiency eliminated even the partial rescue in development of *Rpl22*$^{-/-}$ thymocytes afforded by PUMA deletion alone (Figure 8A). Both total thymic cellularity as well as the proportion and absolute numbers of DP thymocytes were decreased to levels exhibited by mice singly deficient in Rpl22 (Figure 8A). DN subpopulations were not significantly altered, as expected since they remained unchanged even in Rpl22/PUMA-deficient mice (Figure 8B). Evaluation of bromodeoxyuracil (BrdU) incorporation as a means of measuring the number of cells in S phase, revealed that despite their increased expression of p21^{waf}, *Rpl22*$^{-/-}$ DN3 thymocytes actually incorporated more BrdU than *Rpl22*+/+ littermate controls (Figure 8C). Therefore, for reasons that are unclear, Rpl22-deficiency appears to increase the

proliferation of DN3 progenitor cells. It is possible that the increased proliferation of these cells may them more sensitive to p53-induced apoptosis. Consistent with this notion, while we detected only modest changes in the extent of BrdU incorporation between Rpl22/PUMA-double deficient and Rpl22/PUMA/$p21^{waf}$-triple deficient thymocytes (DN4; Figure 8C), triple-deficient thymocytes did exhibit greater levels of apoptosis than did thymocytes from Rpl22/PUMA-double deficient mice in many of the subsets analyzed (Figure 8D). These surprising findings suggest that $p21^{waf}$ was actually functioning to facilitate development in the Rpl22/PUMA-double deficient mice, either through subtly restraining proliferation or by promoting survival, since the additional loss of $p21^{waf}$ resulted in increased cell death.

These data indicate that the p53-mediated developmental block in Rpl22-deficient thymocytes results from the coordinate induction of a constellation of p53 targets, with the pro-apoptotic factors PUMA and Bim, playing predominant roles in enforcing the p53-mediated developmental arrest. Collectively, these p53 effectors are limiting proliferation and survival in a manner distinct from that observed following induction of p53 through other means, such as DNA damage.

Discussion

Rpl22-deficient thymocytes fail to progress beyond the β-selection checkpoint due to the activation of a p53-mediated checkpoint. The importance of this checkpoint in mediating the developmental block is demonstrated by the complete restoration of T cell development upon ablation of *Trp53* in $Rpl22^{-/-}$ thymocytes (Figure 1). Herein we analyzed the downstream p53 effectors responsible for the p53-mediated developmental arrest of $Rpl22^{-/-}$ αβ-lineage precursors. Expression profiling revealed that while many p53 effectors capable of regulating cell growth and survival were induced, few played sufficiently important roles as to alleviate (partially) the developmental block upon removal. Indeed, we found that the expression of a cell cycle inhibitor, $p21^{waf}$, as well as the pro-apoptotic factors PUMA, Bim, Bax, and Noxa were all induced in $Rpl22^{-/-}$ thymocytes. Nevertheless, only elimination of PUMA and Bim resulted in detectable restoration of T cell development, with nearly full restoration of development occurring upon simultaneous elimination of both. Therefore, our results indicate that even within the same tissue, different inductive stimuli (e.g., DNA damage vs. RpL22 deficiency) result in the utilization by p53 of a somewhat distinct set of molecular effectors to limit cell growth and survival.

Our loss-of-function analysis of p53 effectors revealed that elimination of individual p53 molecular effectors had limited ability to alleviate the p53-mediated block and restore development. While not a direct target of p53, Bim expression was elevated in $Rpl22^{-/-}$ DN3 thymocytes. The ability of Bim knockdown to partially restore development of $Rpl22^{-/-}$ thymocytes beyond the β-selection checkpoint to the DP stage is consistent with a report indicating that Bim is an important death effector at this checkpoint, in that Bim deficiency was able to partially restore development of pre-TCR–deficient thymocytes (42). Furthermore, we observed that combined reductions in Bim and PUMA resulted in nearly complete rescue of the development of $Rpl22^{-/-}$ T cell progenitors *in vitro*. The results are in agreement with recent findings that indicate combined Bim, PUMA, and Bid loss prevents direct activation of Bax/Bak-mediated apoptosis (43). Likewise, the failure of Noxa and Bax knockdown to restore development or $Rpl22^{-/-}$ thymocytes is consistent with previously published analyses (44). Noxa is reported to induce apoptosis indirectly by promoting Bax and Bak function and to require oncogene expression (e.g., oncogene E1A) for maximal effect (23). Moreover, because Noxa was also upregulated in $Rpl22^{-/-}$ γδ-lineage cells, which do not show p53 induction or arrested development, we reasoned that Noxa induction might be p53-independent and therefore unlikely to play a major role in the

p53-mediated developmental block at the β-selection checkpoint. Lastly, knockdown of the Bcl-2 family member, Bax, also failed to rescue development, perhaps because the pro-apoptotic function of Bax is reported to be less potent in thymocytes than that of Bim (45), and because Bax deficiency is reported to produce a mild rescue of development block caused by the absence of IL-7 signaling, but is not known to play a major role at the β-selection checkpoint (46). Alternatively, the related pro-apoptotic protein Bak can also form homodimers that result in mitochondrial disruption and cytochrome c efflux, and thus might compensate for Bax loss (47).

It was quite surprising that ablation of the two major p53 effectors controlling cell growth and survival in the thymus, $p21^{waf}$ and PUMA, respectively, not only failed to rescue development completely but also behaved antagonistically when eliminated simultaneously. Indeed, PUMA-deficiency is able to render thymocytes completely resistant to p53-mediated death following exposure to DNA damage (21); however, PUMA-deficiency failed to fully rescue the development of *Rpl22*$^{-/-}$ thymocytes, instead restoring thymic cellularity to only ~10% of normal levels. While co-elimination of Bim and PUMA was able to provide nearly complete rescue of the development of *Rpl22*$^{-/-}$ thymocytes in vitro, presumably due to a complete suppression of p53-mediated apoptosis, co-elimiation of PUMA with cell cycle regulator $p21^{waf}$ not only failed to alleviate the developmental block of *Rpl22*$^{-/-}$ thymocytes but also rendered the developmental block more penetrant, interfering with the ability of PUMA-deficiency to restore development to the DP stage (Figure 8). The mechanistic basis by which $p21^{waf}$ deficiency antagonizes the rescue of development by PUMA-deficiency remains unclear as we detected only modest changes in BrdU incorporation caused by further elimination of $p21^{waf}$ (Figure 8C). Nevertheless, it is possible that even subtle changes in proliferation could be biologically relevant, as cells in cycle have been reported to be more sensitive to p53-mediated apoptosis and PUMA-deficiency may be unable to rescue cells from p53-mediated death in this context (48, 49). Consistent with this possibility, 21^{waf}-deficiency did result in increased apoptosis in many thymocyte subsets from Rpl22/PUMA/$p21^{waf}$-deficient mice. This outcome may be a consequence of the aforementioned subtle effects on proliferation. Alternatively, recent studies have demonstrated an anti-apoptotic role for $p21^{waf}$ under certain cell stress conditions (50–53). The greater sensitivity of proliferating cells to cell death may also play an important role in rendering αβ lineage cells more sensitive to developmental block in *Rpl22–/–* mice (7). Indeed, we also made the surprising observation that despite expressing higher levels of $p21^{waf}$, *Rpl22*$^{-/-}$ thymocytes incorporated more BrdU than their wild type littermates. The mechanistic basis for this is unclear but is under active investigation. Moreover, αβ lineage progenitors are thought to undergo much more extensive proliferation than do γδ lineage progenitors (54, 55) and this may contribute to their increased sensitivity to development arrest due upon loss of Rpl22.

The cause of p53 induction in *Rpl22*$^{-/-}$ thymocytes remains unclear, but we have shown that it is associated with increased p53 synthesis, not a change in turnover (7). Because we observe p53 induction in *Rpl22*$^{-/-}$*Rag2*$^{-/-}$ thymocytes, it does not result from the Rag2-mediated DNA cleavage events associated with TCR gene rearrangements. Moreover, the absence of a change in p53 stability suggests it is not due to other forms of DNA damage, consistent with the incomplete dependence of the resulting cell death on PUMA (21). Instead, our current hypothesis is that induction of p53 in *Rpl22*$^{-/-}$ αβ lineage cells results from stress that is a consequence of the proliferative burst accompanying pre-TCR stimulation at the DN3 stage. This idea is consistent with the developmental block in *Rpl22*$^{-/-}$ thymocytes being selective to those of the αβ lineage, since these cells undergo a robust proliferative expansion following pre-TCR signaling, than does not occur during development of γδ lineage progenitors (54, 55). In agreement, we observed a transient induction of p53 following acute, mitogenic anti-CD3 stimulation of Rpl22-expressing

Rag2$^{-/-}$ thymocytes, which mimics pre-TCR stimulation (7) (Figure 3). We think the reason that p53 induction is normally transient is because pre-TCR signaling induces Rpl22 expression, which then returns p53 levels to baseline by repressing p53 synthesis. We hypothesize that p53 induction is sustained in *Rpl22*$^{-/-}$ αβ lineage cells, because Rpl22 is not present and so is incapable of repressing p53 translation. Nevertheless, it is possible that there are normal circumstances where p53 induction might be sustained, such as when the Notch signals upon which development of αβ lineage cells depend are unavailable. Indeed, since Notch signaling has been reported to repress p53 (and induce Rpl22)(56, 57), it is tempting to speculate that the absence of Notch signals could selectively eliminate αβ lineage cells through sustained p53-induction, since γδTCR+ thymocytes develop in a Notch-independent manner (58).

Our findings reveal that p53 induction in *Rpl22*$^{-/-}$ αβ lineage thymocytes impairs their development through multiple molecular effectors controlling growth and survival. The particular effectors employed appear to differ depending on the circumstances surrounding p53 activation. Indeed, while the p53 effector Noxa functions in the context of oncogene induction, PUMA is almost solely responsible for p53-mediated death following DNA-damage. In contrast, multiple direct and indirect p53 effectors (PUMA, miR-34a, Bim and perhaps others) are employed to impair development of *Rpl22*$^{-/-}$ thymocytes. Efforts to address the basis for the selective induction of p53 in *Rpl22*$^{-/-}$ αβ lineage cells and how this influences the constellation of effector molecules controlling growth and survival are in progress.

Acknowledgments

We thank Dr. Maureen Murphy for critical review of the manuscript and thank the following core facilities at Fox Chase Cancer Center for vital support: Biomarker, Cell Culture, DNA Sequencing, DNA Synthesis, Flow Cytometry, and Laboratory Animals.

References

1. Hoffman ES, Passoni L, Crompton T, Leu TM, Schatz DG, Koff A, Owen MJ, Hayday AC. Productive T-cell receptor beta-chain gene rearrangement: coincident regulation of cell cycle and clonality during development in vivo. Genes Dev. 1996; 10:948–962. [PubMed: 8608942]
2. Kruisbeek AM, Haks MC, Carleton M, Michie AM, Zuniga-Pflucker JC, Wiest DL. Branching out to gain control: how the pre-TCR is linked to multiple functions. Immunol Today. 2000; 21:637–644. [PubMed: 11114425]
3. von Boehmer H. Unique features of the pre-T-cell receptor alpha-chain: not just a surrogate. Nat Rev Immunol. 2005; 5:571–577. [PubMed: 15999096]
4. Michie AM, Zuniga-Pflucker JC. Regulation of thymocyte differentiation: pre-TCR signals and beta-selection. Semin Immunol. 2002; 14:311–323. [PubMed: 12220932]
5. Aifantis I, Mandal M, Sawai K, Ferrando A, Vilimas T. Regulation of T-cell progenitor survival and cell-cycle entry by the pre-T-cell receptor. Immunol Rev. 2006; 209:159–169. [PubMed: 16448541]
6. Koltsova EK, Ciofani M, Benezra R, Miyazaki T, Clipstone N, Zuniga-Pflucker JC, Wiest DL. Early growth response 1 and NF-ATc1 act in concert to promote thymocyte development beyond the beta-selection checkpoint. J Immunol. 2007; 179:4694–4703. [PubMed: 17878368]
7. Anderson SJ, Lauritsen JP, Hartman MG, Foushee AM, Lefebvre JM, Shinton SA, Gerhardt B, Hardy RR, Oravecz T, Wiest DL. Ablation of ribosomal protein L22 selectively impairs alphabeta T cell development by activation of a p53-dependent checkpoint. Immunity. 2007; 26:759–772. [PubMed: 17555992]
8. Lavergne JP, Marzouki A, Reboud JP, Reboud AM. Reconstitution of the active rat liver 60 S ribosomal subunit from different preparations of core particles and split proteins. FEBS Lett. 1988; 236:345–351. [PubMed: 3044828]

9. Lavergne JP, Conquet F, Reboud JP, Reboud AM. Role of acidic phosphoproteins in the partial reconstitution of the active 60 S ribosomal subunit. FEBS Lett. 1987; 216:83–88. [PubMed: 3582668]
10. Draptchinskaia N, Gustavsson P, Andersson B, Pettersson M, Willig TN, Dianzani I, Ball S, Tchernia G, Klar J, Matsson H, Tentler D, Mohandas N, Carlsson B, Dahl N. The gene encoding ribosomal protein S19 is mutated in Diamond-Blackfan anaemia. Nat Genet. 1999; 21:169–175. [PubMed: 9988267]
11. Ruggero D, Pandolfi PP. Does the ribosome translate cancer? Nat Rev Cancer. 2003; 3:179–192. [PubMed: 12612653]
12. Wool IG. Extraribosomal functions of ribosomal proteins. Trends Biochem Sci. 1996; 21:164–165. [PubMed: 8871397]
13. Fumagalli S, Di Cara A, Neb-Gulati A, Natt F, Schwemberger S, Hall J, Babcock GF, Bernardi R, Pandolfi PP, Thomas G. Absence of nucleolar disruption after impairment of 40S ribosome biogenesis reveals an rpL11-translation-dependent mechanism of p53 induction. Nat Cell Biol. 2009; 11:501–508. [PubMed: 19287375]
14. Lohrum MA, Ludwig RL, Kubbutat MH, Hanlon M, Vousden KH. Regulation of HDM2 activity by the ribosomal protein L11. Cancer Cell. 2003; 3:577–587. [PubMed: 12842086]
15. Dai MS, Lu H. Inhibition of MDM2-mediated p53 ubiquitination and degradation by ribosomal protein L5. J Biol Chem. 2004; 279:44475–44482. [PubMed: 15308643]
16. Ofir-Rosenfeld Y, Boggs K, Michael D, Kastan MB, Oren M. Mdm2 regulates p53 mRNA translation through inhibitory interactions with ribosomal protein L26. Mol Cell. 2008; 32:180–189. [PubMed: 18951086]
17. Takagi M, Absalon MJ, McLure KG, Kastan MB. Regulation of p53 translation and induction after DNA damage by ribosomal protein L26 and nucleolin. Cell. 2005; 123:49–63. [PubMed: 16213212]
18. Willis SN, Adams JM. Life in the balance: how BH3-only proteins induce apoptosis. Curr Opin Cell Biol. 2005; 17:617–625. [PubMed: 16243507]
19. Bouillet P, Metcalf D, Huang DC, Tarlinton DM, Kay TW, Kontgen F, Adams JM, Strasser A. Proapoptotic Bcl-2 relative Bim required for certain apoptotic responses, leukocyte homeostasis, and to preclude autoimmunity. Science. 1999; 286:1735–1738. [PubMed: 10576740]
20. Erlacher M, Michalak EM, Kelly PN, Labi V, Niederegger H, Coultas L, Adams JM, Strasser A, Villunger A. BH3-only proteins Puma and Bim are rate-limiting for gamma-radiation- and glucocorticoid-induced apoptosis of lymphoid cells in vivo. Blood. 2005; 106:4131–4138. [PubMed: 16118324]
21. Jeffers JR, Parganas E, Lee Y, Yang C, Wang J, Brennan J, MacLean KH, Han J, Chittenden T, Ihle JN, McKinnon PJ, Cleveland JL, Zambetti GP. Puma is an essential mediator of p53-dependent and -independent apoptotic pathways. Cancer Cell. 2003; 4:321–328. [PubMed: 14585359]
22. Villunger A, Scott C, Bouillet P, Strasser A. Essential role for the BH3-only protein Bim but redundant roles for Bax, Bcl-2, and Bcl-w in the control of granulocyte survival. Blood. 2003; 101:2393–2400. [PubMed: 12433687]
23. Shibue T, Takeda K, Oda E, Tanaka H, Murasawa H, Takaoka A, Morishita Y, Akira S, Taniguchi T, Tanaka N. Integral role of Noxa in p53-mediated apoptotic response. Genes Dev. 2003; 17:2233–2238. [PubMed: 12952892]
24. Deng C, Zhang P, Harper JW, Elledge SJ, Leder P. Mice lacking p21CIP1/WAF1 undergo normal development, but are defective in G1 checkpoint control. Cell. 1995; 82:675–684. [PubMed: 7664346]
25. Di Micco R, Cicalese A, Fumagalli M, Dobreva M, Verrecchia A, Pelicci PG, di Fagagna F. DNA damage response activation in mouse embryonic fibroblasts undergoing replicative senescence and following spontaneous immortalization. Cell Cycle. 2008; 7:3601–3606. [PubMed: 19001874]
26. el-Deiry WS, Tokino T, Velculescu VE, Levy DB, Parsons R, Trent JM, Lin D, Mercer WE, Kinzler KW, Vogelstein B. WAF1, a potential mediator of p53 tumor suppression. Cell. 1993; 75:817–825. [PubMed: 8242752]

27. Raver-Shapira N, Marciano E, Meiri E, Spector Y, Rosenfeld N, Moskovits N, Bentwich Z, Oren M. Transcriptional activation of miR-34a contributes to p53-mediated apoptosis. Mol Cell. 2007; 26:731–743. [PubMed: 17540598]
28. Shibue T, Suzuki S, Okamoto H, Yoshida H, Ohba Y, Takaoka A, Taniguchi T. Differential contribution of Puma and Noxa in dual regulation of p53-mediated apoptotic pathways. EMBO J. 2006; 25:4952–4962. [PubMed: 17024184]
29. Shinkai Y, Rathbun G, Lam K-P, Oltz EM, Stewart V, Mendelsohn M, Charron J, Datta M, Young F, Stall AM, Alt FW. RAG-2-deficient mice lack mature lymphocytes owing to inability to initiate V(D)J recombination. Cell. 1992; 68:855–867. [PubMed: 1547487]
30. Fehling HJ, Krotkova A, Saint-Ruf C, von Boehmer H. Crucial role of the pre-T-cell receptor alpha gene in development of alpha beta but not gamma delta T cells [published erratum appears in Nature 1995 Nov 23;378(6555):419]. Nature. 1995; 375:795–798. [PubMed: 7596413]
31. Jacks T, Remington L, Williams BO, Schmitt EM, Halachmi S, Bronson RT, Weinberg RA. Tumor spectrum analysis in p53-mutant mice. Curr Biol. 1994; 4:1–7. [PubMed: 7922305]
32. Dickins RA, Hemann MT, Zilfou JT, Simpson DR, Ibarra I, Hannon GJ, Lowe SW. Probing tumor phenotypes using stable and regulated synthetic microRNA precursors. Nat Genet. 2005; 37:1289–1295. [PubMed: 16200064]
33. Fehling HJ, Iritani BM, Krotkova A, Forbush KA, Laplace C, Perlmutter RM, von Boehmer H. Restoration of thymopoiesis in pT alpha−/− mice by anti-CD3epsilon antibody treatment or with transgenes encoding activated Lck or tailless pT alpha. Immunity. 1997; 6:703–714. [PubMed: 9208843]
34. Fehling HJ, Krotkova A, Saint-Ruf C, von Boehmer H. Crucial role of the pre-T-cell receptor alpha gene in development of alpha beta but not gamma delta T cells. Nature. 1995; 375:795–798. [PubMed: 7596413]
35. Surh CD, Sprent J. T-cell apoptosis detected in situ during positive and negative selection in the thymus. Nature. 1994; 372:100–103. [PubMed: 7969401]
36. Shinkai Y, Alt FW. CD3 epsilon-mediated signals rescue the development of CD4+CD8+ thymocytes in RAG-2−/− mice in the absence of TCR beta chain expression. Int Immunol. 1994; 6:995–1001. [PubMed: 7947468]
37. Azzam HS, Grinberg A, Lui K, Shen H, Shores EW, Love PE. CD5 expression is developmentally regulated by T cell receptor (TCR) signals and TCR avidity. Journal of Experimental Medicine. 1998; 188:2301–2311. [PubMed: 9858516]
38. He L, He X, Lim LP, de Stanchina E, Xuan Z, Liang Y, Xue W, Zender L, Magnus J, Ridzon D, Jackson AL, Linsley PS, Chen C, Lowe SW, Cleary MA, Hannon GJ. A microRNA component of the p53 tumour suppressor network. Nature. 2007; 447:1130–1134. [PubMed: 17554337]
39. Tarasov V, Jung P, Verdoodt B, Lodygin D, Epanchintsev A, Menssen A, Meister G, Hermeking H. Differential regulation of microRNAs by p53 revealed by massively parallel sequencing: miR-34a is a p53 target that induces apoptosis and G1-arrest. Cell Cycle. 2007; 6:1586–1593. [PubMed: 17554199]
40. Schmitt TM, Zuniga-Pflucker JC. Induction of T cell development from hematopoietic progenitor cells by delta-like-1 in vitro. Immunity. 2002; 17:749–756. [PubMed: 12479821]
41. Brugarolas J, Chandrasekaran C, Gordon JI, Beach D, Jacks T, Hannon GJ. Radiation-induced cell cycle arrest compromised by p21 deficiency. Nature. 1995; 377:552–557. [PubMed: 7566157]
42. Mandal M, Crusio KM, Meng F, Liu S, Kinsella M, Clark MR, Takeuchi O, Aifantis I. Regulation of lymphocyte progenitor survival by the proapoptotic activities of Bim and Bid. Proc Natl Acad Sci U S A. 2008; 105:20840–20845. [PubMed: 19088189]
43. Ren D, Tu HC, Kim H, Wang GX, Bean GR, Takeuchi O, Jeffers JR, Zambetti GP, Hsieh JJ, Cheng EH. BID, BIM, and PUMA are essential for activation of the BAX- and BAK-dependent cell death program. Science. 330:1390–1393. [PubMed: 21127253]
44. Michalak E, Villunger A, Erlacher M, Strasser A. Death squads enlisted by the tumour suppressor p53. Biochem Biophys Res Commun. 2005; 331:786–798. [PubMed: 15865934]
45. Hutcheson J, Scatizzi JC, Siddiqui AM, Haines GK 3rd, Wu T, Li QZ, Davis LS, Mohan C, Perlman H. Combined deficiency of proapoptotic regulators Bim and Fas results in the early onset of systemic autoimmunity. Immunity. 2008; 28:206–217. [PubMed: 18275831]

46. Khaled AR, Li WQ, Huang J, Fry TJ, Khaled AS, Mackall CL, Muegge K, Young HA, Durum SK. Bax deficiency partially corrects interleukin-7 receptor alpha deficiency. Immunity. 2002; 17:561–573. [PubMed: 12433363]
47. Strasser A. The role of BH3-only proteins in the immune system. Nat Rev Immunol. 2005; 5:189–200. [PubMed: 15719025]
48. Komarova EA, Christov K, Faerman AI, Gudkov AV. Different impact of p53 and p21 on the radiation response of mouse tissues. Oncogene. 2000; 19:3791–3798. [PubMed: 10949934]
49. Komarova EA, Kondratov RV, Wang K, Christov K, Golovkina TV, Goldblum JR, Gudkov AV. Dual effect of p53 on radiation sensitivity in vivo: p53 promotes hematopoietic injury, but protects from gastro-intestinal syndrome in mice. Oncogene. 2004; 23:3265–3271. [PubMed: 15064735]
50. Gartel AL, Radhakrishnan SK. Lost in transcription: p21 repression, mechanisms, and consequences. Cancer Res. 2005; 65:3980–3985. [PubMed: 15899785]
51. Villeneuve NF, Sun Z, Chen W, Zhang DD. Nrf2 and p21 regulate the fine balance between life and death by controlling ROS levels. Cell Cycle. 2009; 8:3255–3256. [PubMed: 19806015]
52. Chen W, Sun Z, Wang XJ, Jiang T, Huang Z, Fang D, Zhang DD. Direct interaction between Nrf2 and p21(Cip1/WAF1) upregulates the Nrf2-mediated antioxidant response. Mol Cell. 2009; 34:663–673. [PubMed: 19560419]
53. Sohn D, Essmann F, Schulze-Osthoff K, Janicke RU. p21 blocks irradiation-induced apoptosis downstream of mitochondria by inhibition of cyclin-dependent kinase-mediated caspase-9 activation. Cancer Res. 2006; 66:11254–11262. [PubMed: 17145870]
54. Prinz I, Sansoni A, Kissenpfennig A, Ardouin L, Malissen M, Malissen B. Visualization of the earliest steps of gammadelta T cell development in the adult thymus. Nat Immunol. 2006; 7:995–1003. [PubMed: 16878135]
55. Taghon T, Yui MA, Pant R, Diamond RA, Rothenberg EV. Developmental and molecular characterization of emerging beta- and gammadelta-selected pre-T cells in the adult mouse thymus. Immunity. 2006; 24:53–64. [PubMed: 16413923]
56. Beverly LJ, Felsher DW, Capobianco AJ. Suppression of p53 by Notch in lymphomagenesis: implications for initiation and regression. Cancer Res. 2005; 65:7159–7168. [PubMed: 16103066]
57. Chan SM, Weng AP, Tibshirani R, Aster JC, Utz PJ. Notch signals positively regulate activity of the mTOR pathway in T-cell acute lymphoblastic leukemia. Blood. 2007; 110:278–286. [PubMed: 17363738]
58. Ciofani M, Knowles GC, Wiest DL, von Boehmer H, Zuniga-Pflucker JC. Stage-specific and differential notch dependency at the alphabeta and gammadelta T lineage bifurcation. Immunity. 2006; 25:105–116. [PubMed: 16814577]

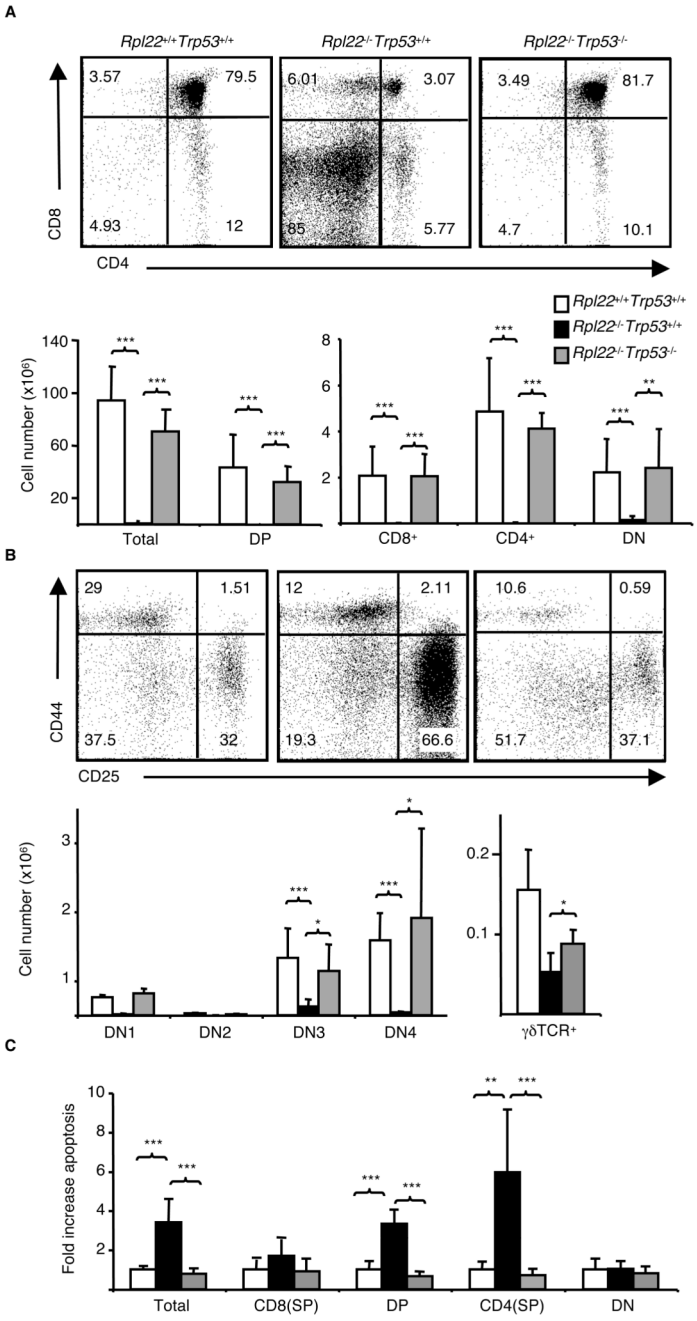

Figure 1.

Trp53 deletion restores development to Rpl22-deficient mice. (A) Single cell suspensions of thymocytes from mice with the indicated genotypes are shown. FACS plots show CD4 and CD8 expression on thymocytes that were gated on doublet excluded, live lymphocytes. Cell numbers were calculated by multiplying the absolute cell number of the thymus by the fraction of each indicated subset identified by FACS analysis. Bar graphs show the mean of the absolute cell number ± s.d. (B) Gated DN thymocytes from mice used in (A) were stained with anti-CD25 and CD44 to reveal DN fractions. Bar graphs show the mean of the absolute cell numbers ± s.d. for the indicated subsets (C) Annexin V binding and PI staining on total thymocytes. Bar graphs show the mean of the fold increase in apoptosis ± s.d.

within each subset as compared to Rpl22-sufficient T cells. N=5 mice per genotype, per analysis. Results are representative of at least 3 independent experiments. *P-value <0.05, **P-value <0.01,***P-value < 0.001.

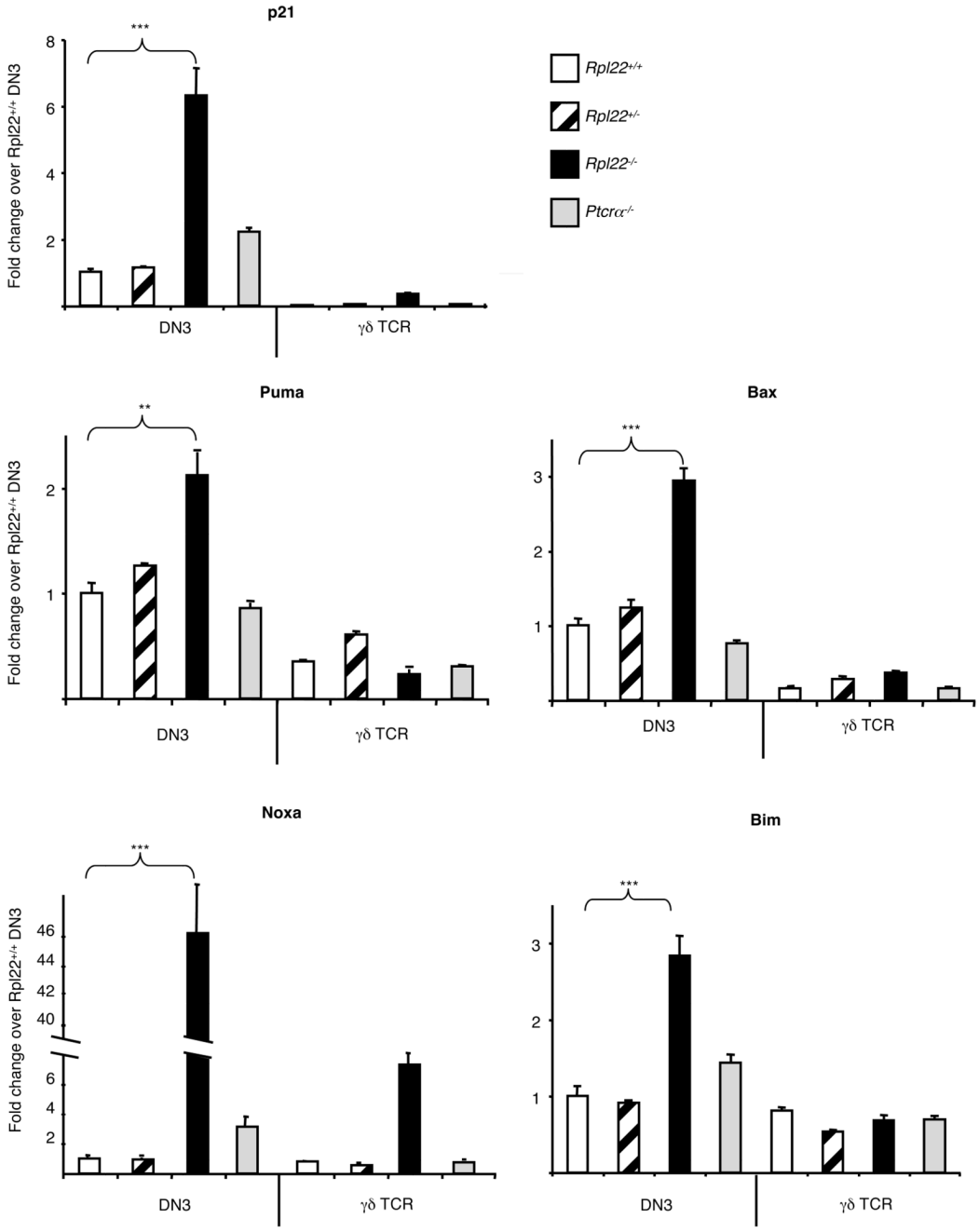

Figure 2.

Quantitative real-time PCR analysis of mRNA encoding p53 targets in αβ- or γδ-lineage thymocytes. Thymocytes were pooled from 12 $Rpl22^{+/+}$, 13 $Rpl22^{-/-}$, or 6 $Rpl22^{+/-}$ mice, and the indicated populations were isolated by flow cytometry and used to generate cDNA: DN3 ($\gamma\delta TCR^{-}CD4^{-}CD8^{-}CD44^{-}CD25^{+}$) or γδ lineage ($CD4^{-}CD8^{-}\gamma\delta TCR^{+}$). Analysis for each primer/probe set was performed for each cell type in triplicate. mRNA levels were normalized to GAPDH. Bar graphs show the fold change ($2^{-\Delta\Delta Ct}$ or RQ value + RQ max) over *Rpl22*$^{+/+}$ DN3 cells. Results are representative of two independent experiments. P values were calculated for triplicate measurements within each experiment. **P-value <0.01, ***P-value <0.001.

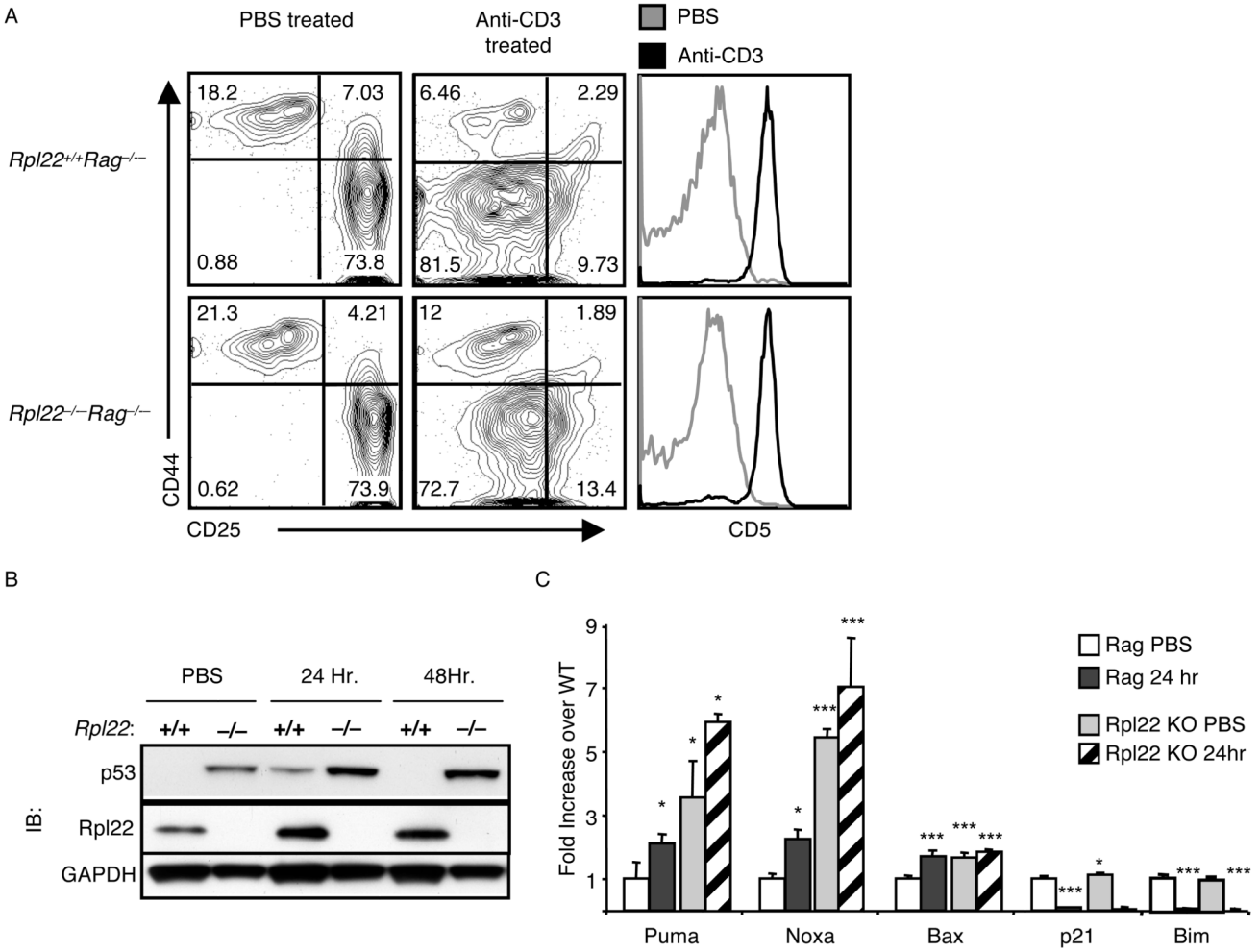

Figure 3.

Analysis of p53 targets following acute mitogenic stimulation of *Rpl22*$^{-/-}$*Rag2*$^{-/-}$ T cell precursors. (A) FACS plots of pooled thymocytes isolated from mice 24 hr after intraperitoneal injection with PBS (control) or anti-CD3 mAb. FACS plots show staining for CD44, CD25, or CD5 within DN (CD4^{-}CD8^{-}) subsets from *Rag2*$^{-/-}$ mice of the indicated genotypes. (B) Detergent extracts of thymocytes isolated from *Rpl22*$^{+/+}$*Rag2*$^{-/-}$ or *Rpl2*$^{-/-}$*Rag2*$^{-/-}$ mice stimulated for the indicated times as in (A) were immunoblotted with anti-p53, RpL22, or GAPDH antibodies. (C) Quantitative real-time PCR analysis of DN thymocytes from mice injected with PBS or anti-CD3 as in (A). Live, DN thymocytes were isolated by flow cytometric-based cell sorting and used to generated cDNA. mRNA levels were normalized to GAPDH. Bar graph indicates fold change ($2^{-\Delta\Delta Ct}$ or RQ) over control treated *Rpl22*$^{+/+}$*Rag2*$^{-/-}$ (plus RQ max). Results are representative of 3 independent experiments. P values were calculated for triplicate measurements within each experiment. *P-value < 0.05; **P-value < 0.01; ***P-value < 0.001.

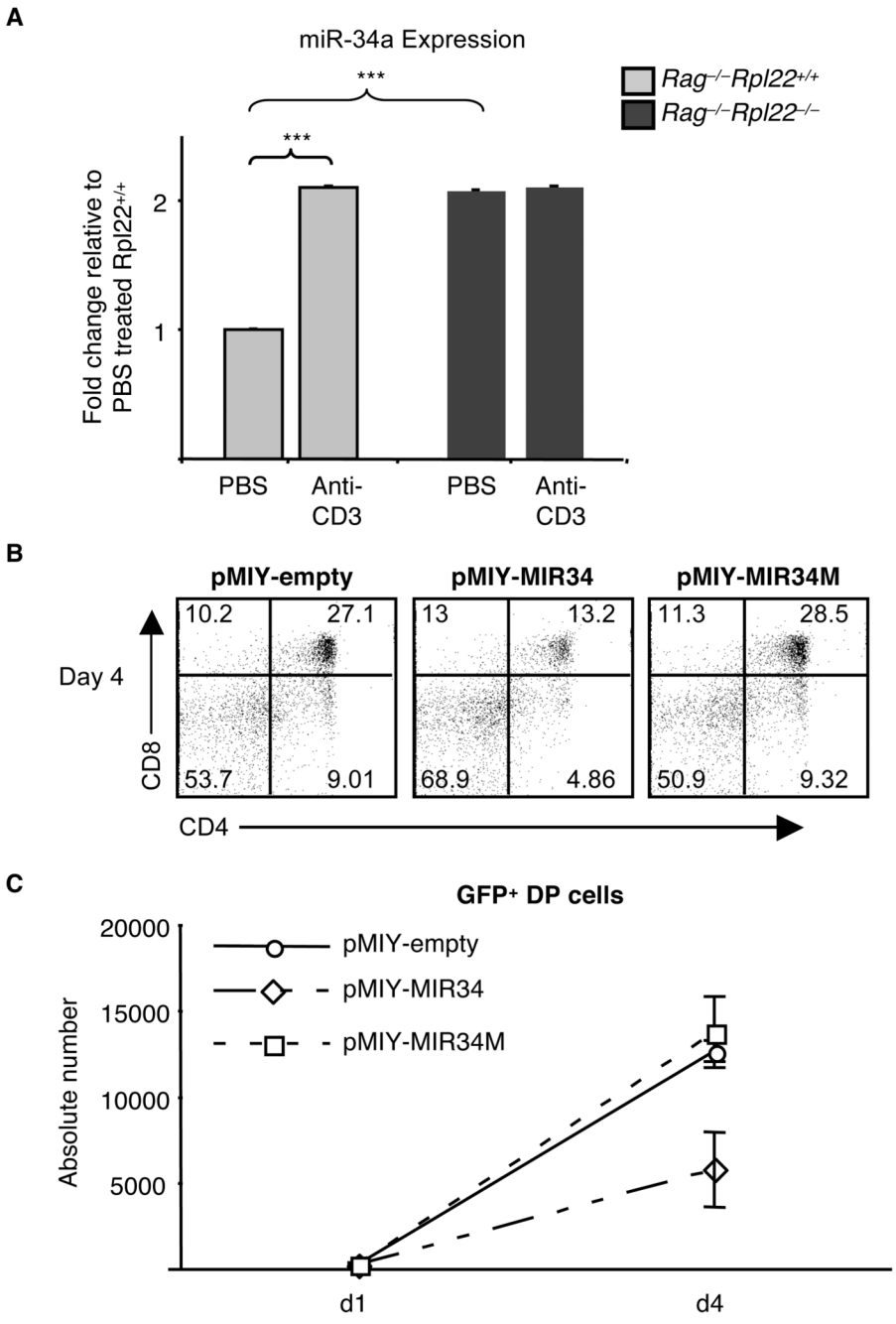

Figure 4.

Enforced expression of miR-34a arrests thymocyte development. (A) Quantitative real-time PCR analysis of miR-34a expression 24 h after intraperitoneal injection of *Rag2*$^{-/-}$ mice of the indicated genotypes with either PBS or anti-CD3. Graphs show mean ± s.d. of the fold increase of mir-34a expression (normalized to small RNA sno-202) from triplicate wells over PBS treated Rpl22$^{+/+}$ DN cells. Results representative of 3 independent experiments. (B–C) Effect of enforced expression of mir-34a on development of thymocytes to the DP stage. DN thymocytes were transduced with miR-34a (pMiY-MIR34) as well as empty vector (pMiY) and mutated mir-34a (pMiY-MIR34M) controls and cultured on OP9-DL1 expressing monolayers. Histograms of gated GFP^{+} cells are depicted in (B). The absolute

number of transduced (GFP^+) DP thymocytes was determined by flow cytometry at the indicated time post transduction and the mean ± s.d. of triplicate wells represented graphically in (C). Results are representative of three independent experiments. P values were calculated for triplicate measurements within each experiment.***p-value<0.001.

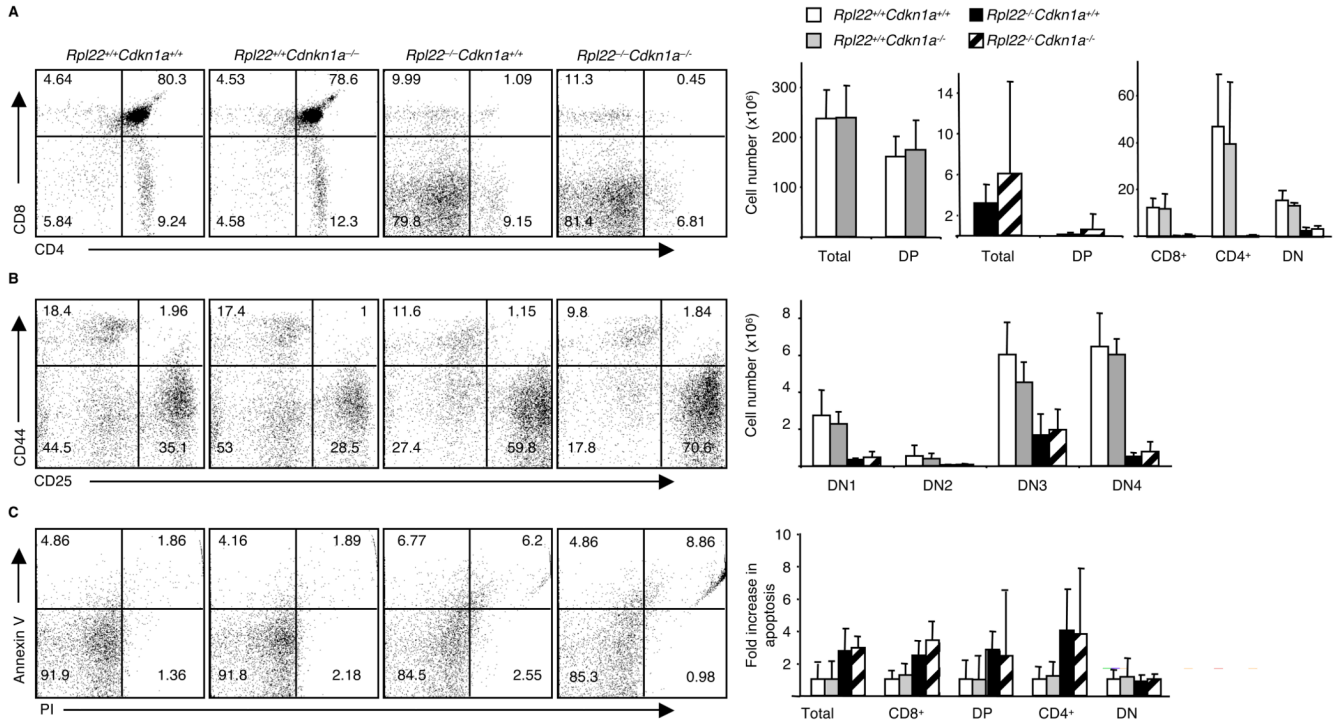

Figure 5.

p21^{waf} deficiency does not restore development to Rpl22-deficient T cells. (A) Histograms depict single cell suspensions of thymocytes from mice with the indicated genotypes stained and gated as in Figure 1. Bar graphs show the mean absolute cell numbers ± s.d. for the indicated thymocyte subsets. (B) FACS analysis of DN subsets from mice in (A). Bar graphs show mean absolute cell number ± s.d. for each DN subset. (C) Total Annexin V and PI staining of thymocytes from (A). The increase in apoptosis is represented graphically showing mean of the fold increase in apoptosis over Rpl22-sufficient thymocytes ± s.d. for each subset. N=5 or more mice from each genotype for each analysis. Results representative of 3 independent experiments.

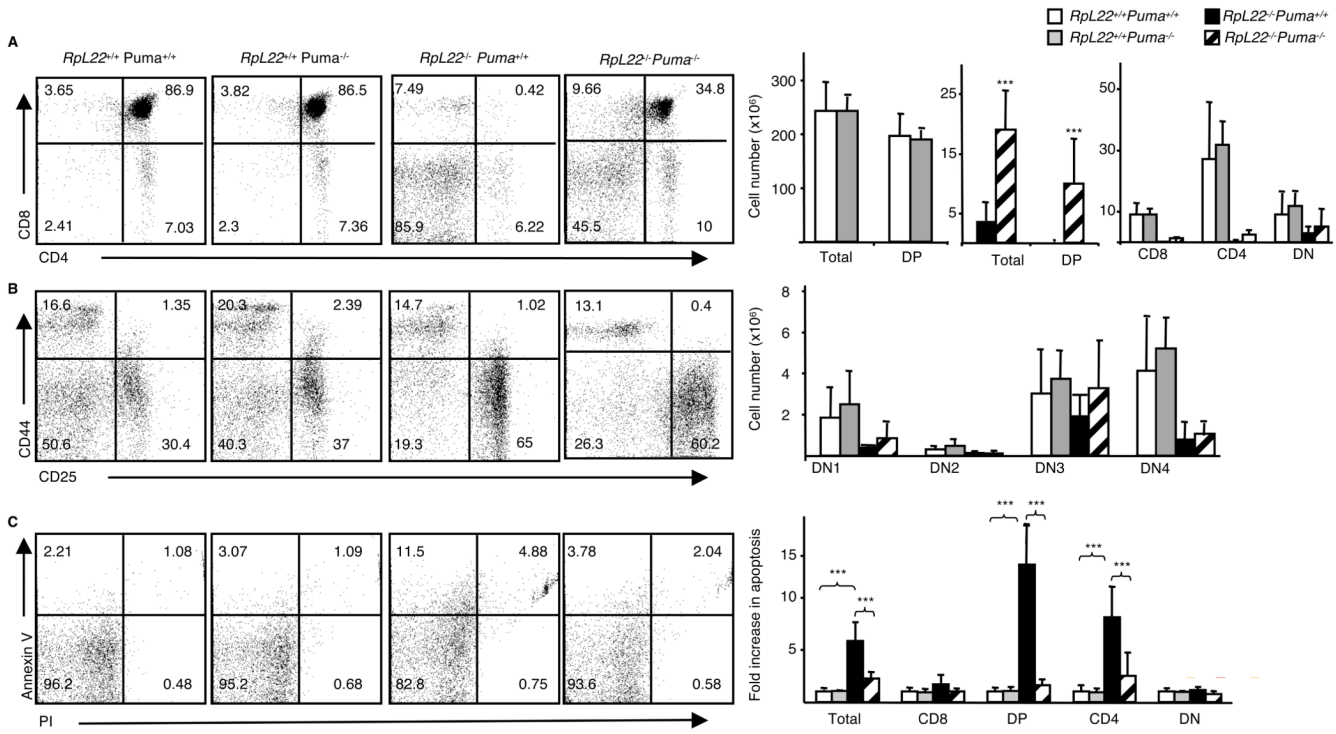

Figure 6.

PUMA-deficiency partially relieves the block in T cell development in Rpl22-deficient mice. Single cell suspensions of thymocytes from mice with the indicated genotypes were subjected to FACS analysis as described in Figure 1. (A) CD4 and CD8 expression on thymocytes from indicated mice. Bar graphs show the mean absolute cell number ± s.d. for each thymocyte subset. (B) Analysis of gated DN subsets from mice with indicated genotypes. Bar graphs show absolute number ± s.d. (C) FACS plots showing Annexin V and PI staining of total thymocytes. Graphs represent the mean of the fold increase in apoptosis over *Rpl22*$^{+/+}$ mice for each thymocyte subset. Results representative of 3 independent experiments. ***p-value<0.001.

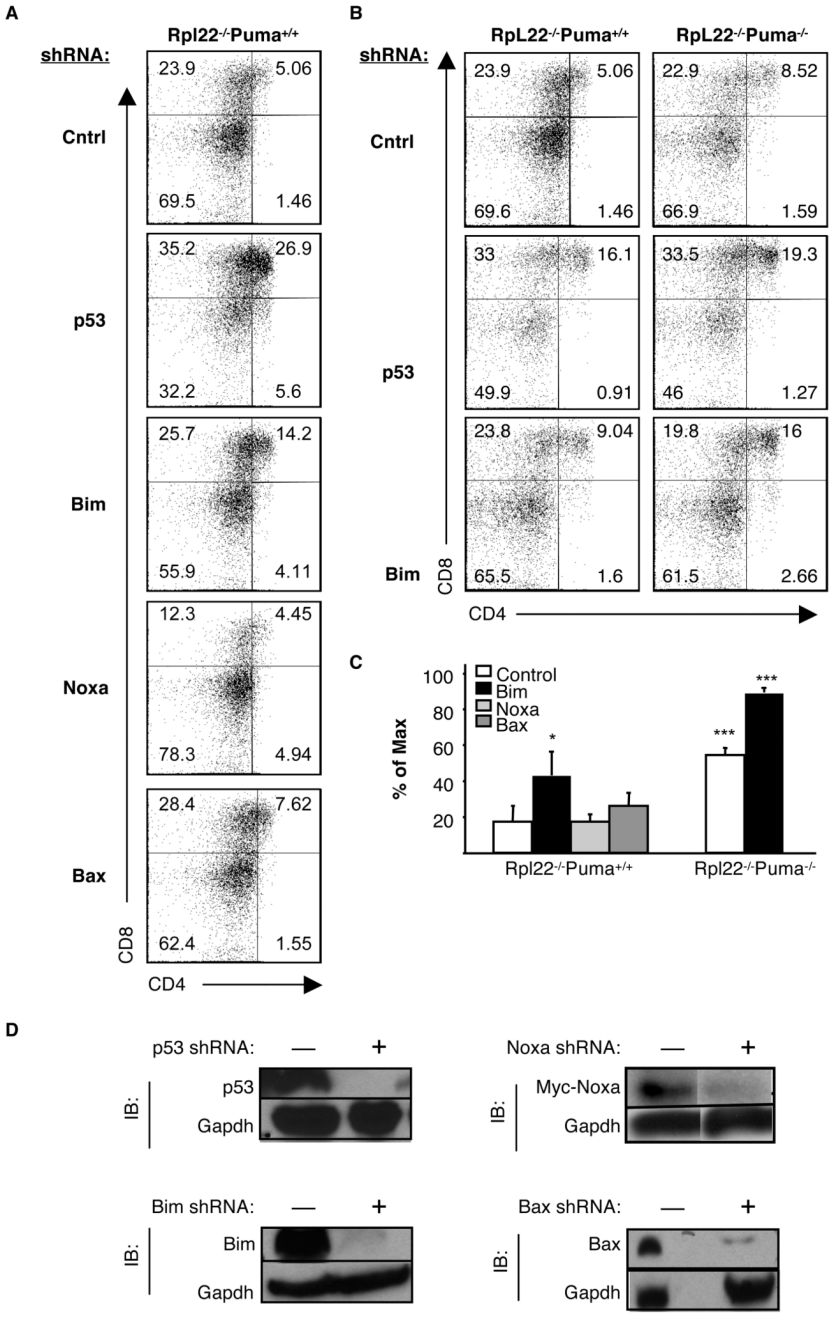

Figure 7.

Co-elimination of Bim and PUMA restores development of αβ lineage RpL22-deficient thymocytes. (A) Effect of single-knockdown of p53 effectors on devopment of *Rpl22*$^{-/-}$ progenitors. Fetal liver progenitors were retrovirally transduced with shRNAs targeting the indicated genes and were cultured on OP9-DL1-bearing monolayers. Developmental progression was assessed by FACS analysis with the indicated antibodies at day 12 post-transduction. Histograms represent gated, GFP+ transduced cells. (B) Fetal liver progenitors from *Rpl22*$^{-/-}$*Puma*$^{+/+}$ or *Rpl22*$^{-/-}$*Puma*$^{-/-}$ mice were transduced with the indicated shRNAs and treated as in (A). Results are representative of 3 independent experiments performed in triplicate wells. (C) Bar graph showing percent of maximum rescue, defined as

the proportion of *Rpl22*$^{-/-}$*Puma*$^{+/+}$ cells reaching the DP stage upon p53 knockdown. Bar graph shows mean ± s.d. of the percent max on day 12 post transduction for cells transduced with control (Cntrl), Bim, Noxa, or Bax shRNA. Statistical student's t-tests is a comparison to *Rpl22*$^{-/-}$*Puma*$^{+/+}$ control shRNA group; *p-value < 0.05, ***p-value < 0.001. (D) Immunoblots verify the extent of target knockdown in Scid.adh thymic lymphoma cells by the shRNAs utilized. Knockdown of Noxa was assessed by co-expressing the Noxa shRNA with a myc-tagged Noxa construct and blotting for the anti-Myc-Tag.

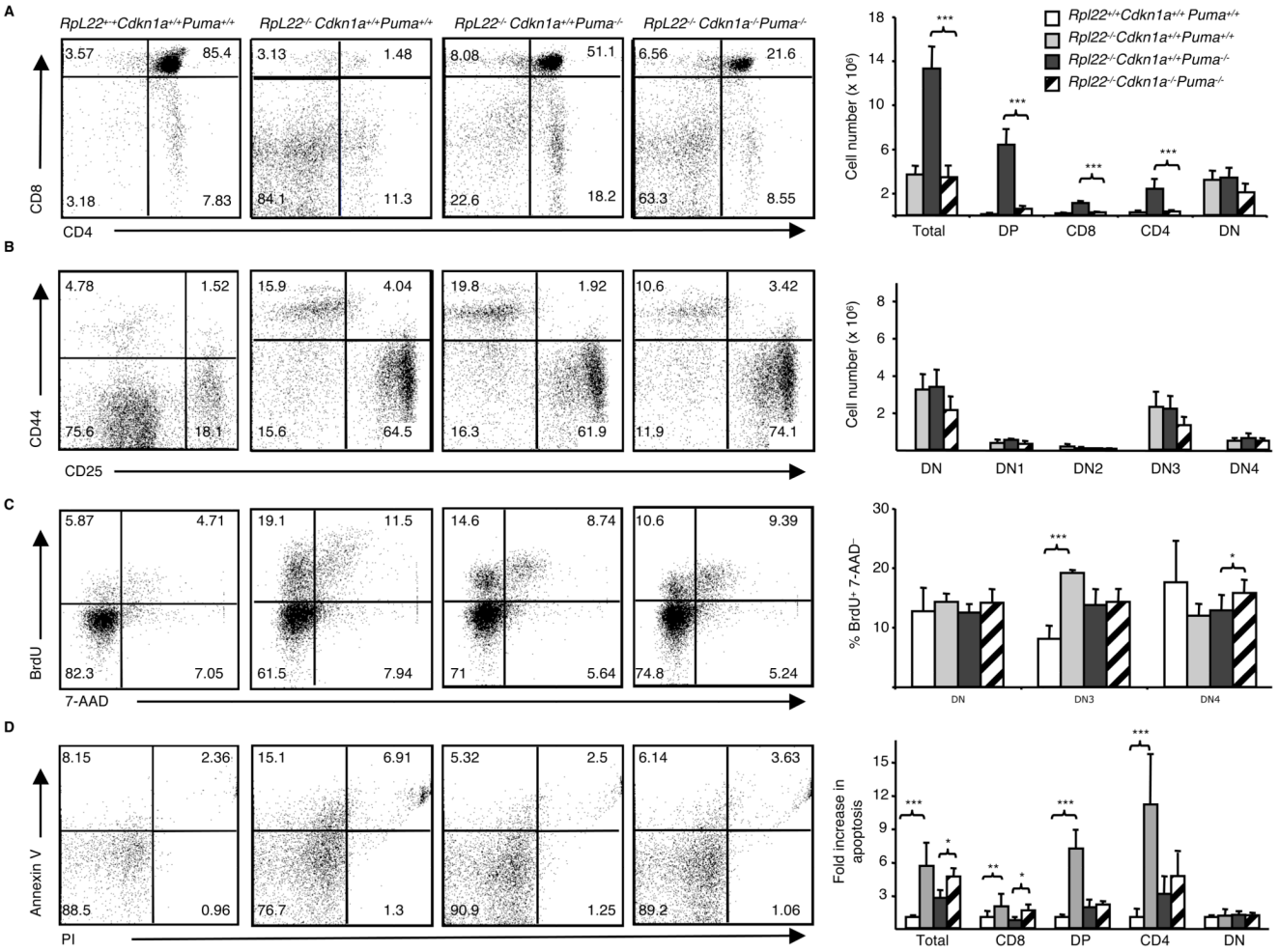

Figure 8.

p21^{waf} deficiency abrogated the rescue of development caused by PUMA-deficiency alone. Single cell suspensions of thymocytes from mice with the indicated genotypes were subjected to FACS analysis. (A) CD4 and CD8 expression on thymocytes. Bar graphs show the mean absolute cell number ± s.d. for each thymocyte. (B) Analysis of DN subsets from mice with indicated genotypes. Bar graphs show absolute number ± s.d. (C) BrdU and 7-AAD staining of DN3 gated thymocytes from wildtype (wt), Rpl22-deficient, Rpl22/PUMA-double deficient or Rpl22/Puma/p21^{waf} triple deficient mice. Bar graphs show the mean of the percentage of BrdU^{+} 7-AAD^{-} cells in DN, DN3, and DN4 subsets ± s.d. N=3 to 5 mice from each genotype from 3-independent experiments. (D) FACS plots showing Annexin V and PI staining of total thymocytes. Graphs represent the mean of the fold increase in apoptosis over RpL22$^{+/+}$ mice for each T cell subset. *p-value >0.5, **p-value >0.01, ***p-value >0.001.